STUDIA UNIVERSITATIS BABEŞ-BOLYAI, CHEMIA, LIV, 4, 2009

MECHANISTIC STUDY OF SE AND GE SEMICONDUCTORS ELECTRODEPOSITION

BOGDAN TUTUNARU[a], ADRIANA SAMIDE[a], MIRCEA PREDA[a]

ABSTRACT. The electrodeposition and mechanism of nucleation of Se and Se-Ge films was studied in this work. The employed experimental techniques were potentiostatic polarization and chronoamperometry. The initial deposition of Se film by potentiostatic polarization shows that the crystallization potential of -0,40 V and corresponding densities linearly depends on the H_2SeO_3 concentration and potential scan rate. The simultaneous presence of both species in the bath composition produced a new peak at -0,50 V. The chronoamperometric study indicate a 3D complex mechanism for Se and Se-Ge electrodeposition. The morphological changes in surface of working electrode was analysed with an Euromex microscope.

Keywords: Semiconductors, Se and Se_2Ge electrodeposition, nucleation mechanism

INTRODUCTION

Selenium is essential for life when consumption of foods contain 0,1 mg kg^{-1} of this element, and is toxic when dietary levels are above 1 mg kg^{-1} [1]. In the human body, selenium is bond by covalent carbon-selenium bonds and some inorganic selenium salts have powerful cancer chemopreventive effects.

Semiconductors were found that they can replace or compete with monocrystalline materials in photoelectrochemical cells [2]. The photo-induced changes observed in semiconductor compounds are attributed to the amorphous state [3]. Selenium has played an important role in the production of metal selenides (ZnSe, MgSe, FeSe, PbSe, SnSe, CdSe etc.) [4-8]. This kind of compounds presents interesting applications such as optical filters, solar cells, laser materials [9,10].

One of the most adequate method to obtain a thin film of semiconductor or metal-selenide compound is electrodeposition [11]. Selenium electrodeposition is a side reaction in the cathodic synthesis of metal selenides [12].

To our knowledge, electrodeposition of Se-Ge has not been reported in the literature. Hence, we have attempted in the present study to deposit a Se-Ge thin film by electrodeposition.

[a] *Faculty of Chemistry, University of Craiova, Calea Bucureşti, no. 107i, Craiova, Romania*

RESULTS AND DISCUSSION

In the electrochemical deposition of Se the electrodeposition potential and the corresponding densities were found to depend on sweep rate and concentration of the electrolyte. Figure 1 shows the cathodic curves obtained in solutions containing H_2SeO_3 at three different concentrations.

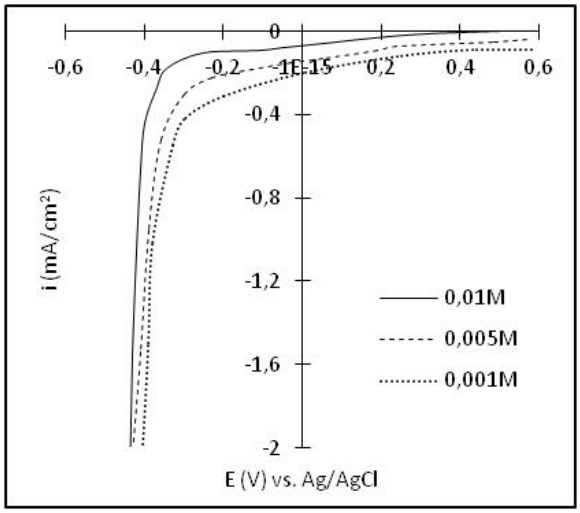

Figure 1. Cathodic curves obtained during selenium deposition onto Pt electrode from 0,01; 0,005 and 0,001 M H_2SeO_3 aqueous solutions, pH=2.

The potential scan was initiated in the negative direction from open circuit potential vs. Ag/AgCl. The reduction wave starts at -0.40 V vs. Ag/AgCl when selenous acid is present in the electrolyte with 0.01 M concentration.

In the case of selenium the crystallization potential and the corresponding current densities linearly depends on the concentration of H_2SeO_3 in solution.

Further analysis at various scan rates (fig. 2) showed clearly a linear variation of the crystallization potential with different scan rate (insert of figure 2).

The current densities are proportional to the scan rate and the crystallization potential is moving to the more positive direction, these features are characteristic for an irreversible system [13,14].

Reduction of the selenium species without the germanium precursor in the electrolyte, starts at -0,4 V vs. Ag/AgCl according to reaction:

$$SeO_3^{2-} + 3H_2O + 4e \rightarrow Se + 6HO^- \quad (E^0 = -0{,}366\ V) \qquad (1)$$

Metallic selenium electrodeposition is also indicated by the purplish colour of the deposit.

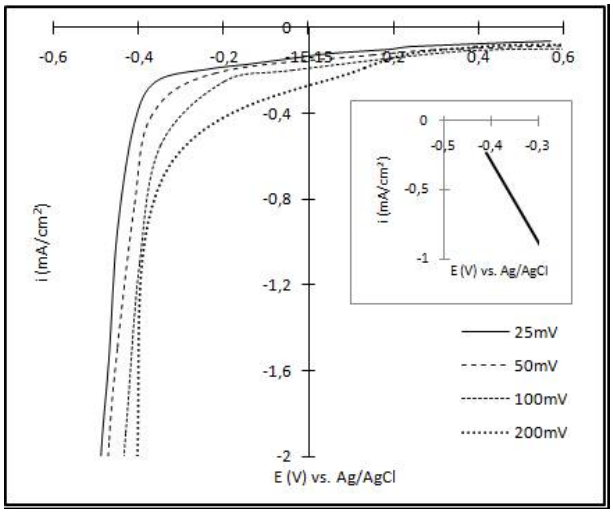

Figure 2. Cathodic polarization curves for Pt electrode at different scan rates in plating bath, H_2SeO_3 0,005 M, pH=2.

We performed a chronoamperometric study in order to examine the nucleation of selenium and selenium-germanium electrodeposition. Figure 3 shows a set of potentiostatic current transients for 0, 10, 30 and 50 mV overcharges obtained during the electrochemical deposition of selenium onto platinum electrode from a 0,005 M H_2SeO_3 solution.

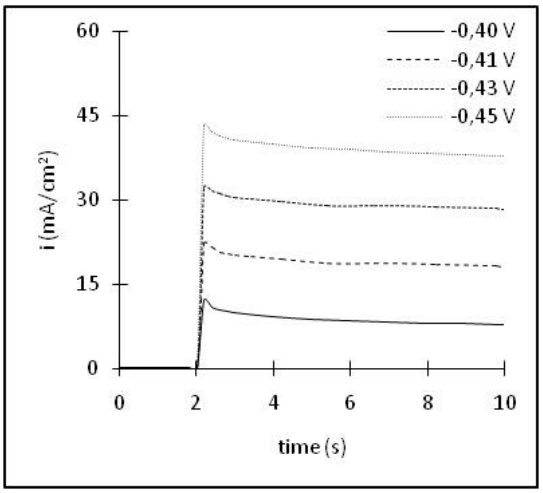

Figure 3. Potentiostatic current transients for the electrodeposition of selenium onto Pt electrode from 0,005 M H_2SeO_3, pH=2.

Experimental current transients are presented in a nondimensional form by ploting i/i_{max} vs. t/t_{max} (2D) and $(i/i_{max})^2$ vs. t/t_{max} (3D) and compared with theoretical values for instantaneous and progressive nucleation, respectively (fig. 4).

As can observe from figure 4, one can affirm that the selenium electrodeposition on the platinum electrode, in the given experimental conditions, take place after a combinatorial kinetic of 3D nucleation.

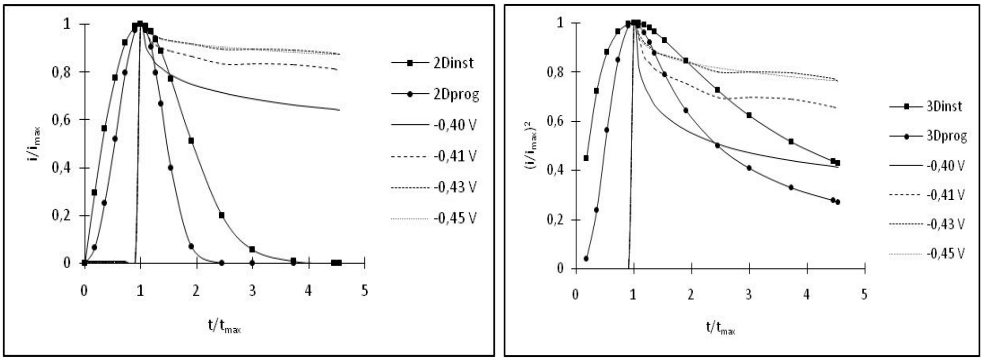

Figure 4. Comparison of the theoretical nondimensional plots for 2D (fig. 4a) and 3D (fig. 4b) for instantaneous and progressive Se nucleation to the experimental current transients in fig. 3.

The simultaneous presence of both species in the bath composition produced noticeable changes in the cathodic response. It can be seen in fig. 5 that a new peak appears during the scan in the negative direction at -0,50 V vs. Ag/AgCl.

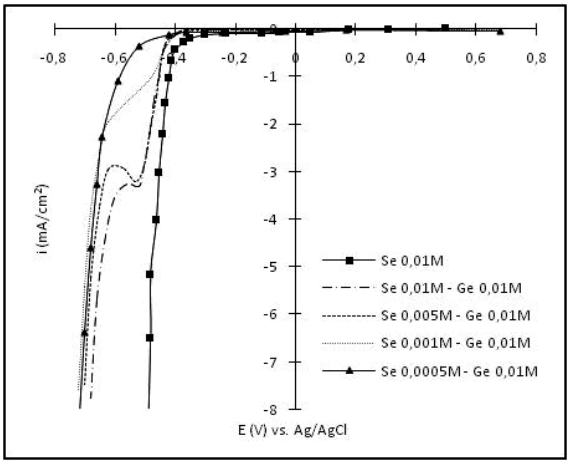

Figure 5. Cathodic curves for Pt electrode obtained during Se and Se-Ge electrodeposition.

We note that the cathodic current densities of this peak are decreasing with the Se concentration decrease. This peak may be ascribed to the formation of Se-Ge on the substrate. The $GeCl_4$ is hydrolyzed with distilled water to produce GeO_2; in this conditions we have to consider the possibility that this peak can be atributed to the GeO_2 reduction to GeO (E^0 = -0.370 V). At more negative potentials further reductions of the deposited selenium to H_2Se and/or germanium species to H_4Ge are possible. Selenium being nobler, it is expected to be deposited first. At selenium concentrations of $5 \cdot 10^{-4}$ M or smaller this peak is not more evident.

The nucleation mechanism of selenium-germanium electrodeposition was study by the chronoamperommetry methode. The corresponding potentiostatic current transients for 0, 10, 30 and 50 mV overpotentials obtained during the electrochemical deposition of selenium-germanium onto platinum electrode from a 0,005 M H_2SeO_3, 0,01 M $GeCl_4$ solution are presented in figure 6.

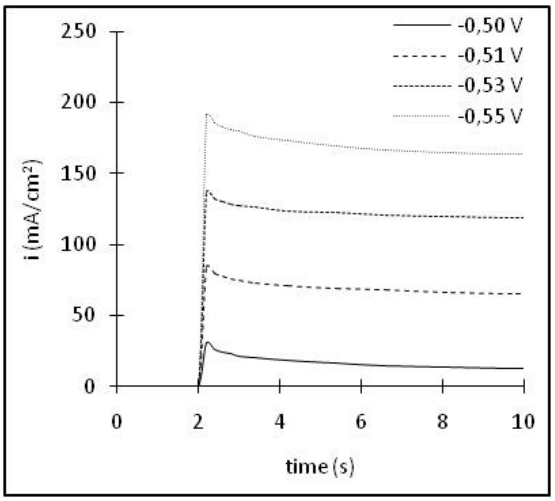

Figure 6. Potentiostatic current transients for the electrodeposition of selenium-germanium onto Pt electrode from 0,005 M H_2SeO_3, 0,01 M $GeCl_4$, pH=2.

From fig. 6 it may be observed that at shorter times there is a maximum current transient that, in this case, can be associated with a process where diffusion-controlled nucleation of selenium and germanium occurs simultaneously at the platinum electrode surface. After this maximum current, in each case the i-t plot passes through a falling current and then approaches to the limiting diffusion current to a planar electrode.

Experimental current transients compared with theoretical one for selenium-germanium instantaneous and progressive nucleation are presented in fig. 7.

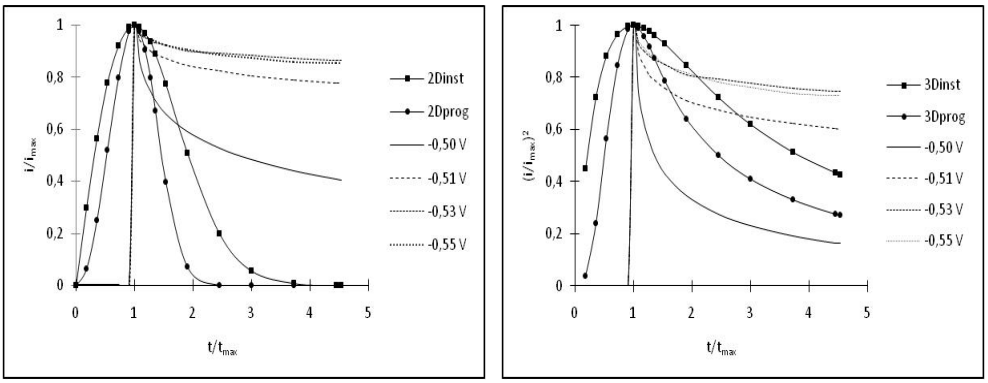

Figure 7. Comparison of the theoretical nondimensional plots for 2D (fig. 7a) and 3D (fig. 7b) for instantaneous and progressive Se-Ge nucleation to the experimental current transients in fig. 6.

Similar to selenium electrodeposition, when the both species are present in the electrolyte composition, at nucleation potential the mechanism fallow the progressive one and at higher overpotentials is changing to instantaneous.

The morphological changes in surface electrode were observed with an Euromex microscope. Figure 8a presents the surface morphology of Pt electrode before electrodeposition; figure 8b presents the surface morphology of deposited selenium and figure 8c presents the selenium-germanium deposit morphology.

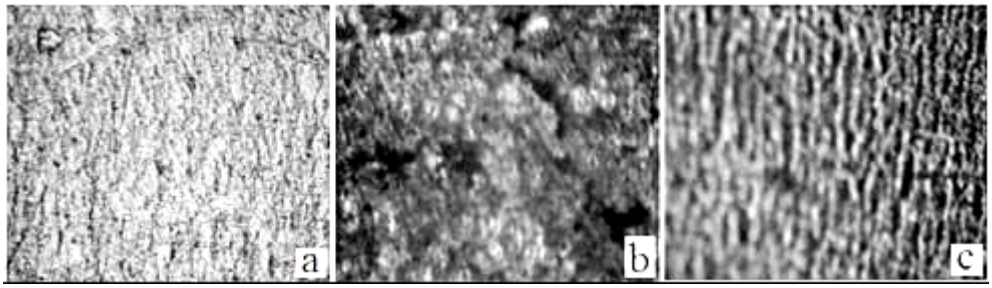

Figure 8. Surface morphology of: Pt electrode before electrodeposition (a), Se (b) and Se-Ge (c) deposited layer.

CONCLUSIONS

The Se and Se-Ge films were deposited onto Pt surface by potentiostatic polarization.

In the electrochemical deposition of Se, the electrodeposition potential and corresponding densities were found to depend on sweep rate and concentration of the electrolyte.

Selenium and selenium-germanium electrodeposition on the platinum electrode, in the given experimental conditions, take place after a combinatorial kinetic of instantaneous and progressive 3D nucleation.

EXPERIMENTAL SECTION

All electrochemical measurements were performed with the Keithley 2420 3A SourceMeter potentiostat/galvanostat. Experimental data recording was carried out in a standard electrochemical cell with three electrodes. The Ag/AgCl, KCl (saturated) was used as the reference electrode to which all potentials are quoted. The working and auxiliary electrodes were made from platinum foils with 1,0 cm^2 geometric area. The Se and Se-Ge films were deposited onto Pt surface by potentiostatic polarization.

All the chemicals used in this work were of analytical grade (99,5%) excepting H_2SeO_3 which was of standard purity (99,99%).

The electrolyte bath for Se deposition comprised of H_2SeO_3 solution, pH = 2 ± 0,05 (by adding HNO_3) and the working temperature was of 20 ± 2 ˚C. The pH of the electrolytic bath was measured using digital pH-meter (HANNA instruments). In order to analyse the influence of H_2SeO_3 concentration, three values of electrolyte concentration were used 0,01; 0,005 and 0,001M.

In the electrolyte bath for Se-Ge electrodeposition, the concentration of H_2SeO_3 was varied from 0,01M to 0,005; 0,001 and 0,0005M while the concentration of $GeCl_4$ was kept constant at 0,01M.

The chronoamperometry methode was used to analyse the nucleation mechanism of Se and Se-Ge electrodeposition.

After the deposition, the films were washed, dried and their morphology were analysed by an Euromex microscope.

REFERENCES

1. O. Wada, N. Kurihara, N. Yamazaki, *Jap. J. Nutr. Assesss.*,**1993**, *10*, 199.
2. V. Plaskov, Solar Energy Conversion, Springer, Berlin, **1990**.
3. P. Nagels, E. Sleeckx, R. Callaerts, L. Tichy, *Solid Stade Commun.*, **1995**, *94*, 49.
4. R. Kowalik, P. Zabinski, K. Fitzner, *Electrochim. Acta*, **2008**, *53*, 6148.
5. T. Mahaligam, A. Kathalingam, C. Sanjeeviraja, R. Chandramohan, J.P. Chu, Y.D. Kim, S. Velumani, *Materials Characterization*, **2007**, *58*, 735.
6. S. Thanikaikarasan, T. Mahalingam, S. Sundaram, A. Kathalingam, Y.D. Kim, T. Kim, *Vacuum*, **2009**, *83*, 1066.
7. M.F. Cabral, H.B. Suffredini, V.A. Perosa, S.T. Tanimoto, S.A.S. Machado, *Appl. Surf. Sci.*, **2008**, *254*, 5612.

8. Z. Zainal, A.J. Ali, A. Kasim, M.Z. Hussein, *Solar Energy & Solar Cells*, **2003**, *79*, 125.
9. W.Z. Wang, Y. Geng, P. Yan, F.Y. Liu, Y. Xie, Y.T. Qian, *J. Am. Chem. Soc.*, **1999**, *121*, 4062.
10. W.B. Zhao, J.J. Zhu, H.Y. Chen, *J. Cryst. Growth*, **2003**, *252*, 587.
11. K. Rajeshwar, *Adv. Mater.*, **1992**, *4*, 1.
12. M.S. Kazacos, B. Miller, *J. Electrochem. Soc.*, **1980**, *127*, 869.
13. Southampton Electrochemitry Group, Instrumental Methods in Electrochemistry, Ellis Horwood, Chichester, UK, **1985**.
14. R.H. Wopschall, I. Shain, *Anal. Chem.*, **1976**, *39*, 1514.